GEOPHYSICS, VOL. 74, NO. 4 (JULY-AUGUST 2009); P. R49–R57, 11 FIGS., 1 TABLE.
10.1190/1.3148002

Thin-bed prestack spectral inversion

J. Germán Rubino[1] and Danilo Velis[1]

ABSTRACT

Prestack seismic data has been used in a new method to fully determine thin-bed properties, including the estimation of its thickness, P- and S-wave velocities, and density. The approach requires neither phase information nor normal-moveout (NMO) corrections, and assumes that the prestack seismic response of the thin layer can be isolated using an offset-dependent time window. We obtained the amplitude-versus-angle (AVA) response of the thin bed considering converted P-waves, S-waves, and all the associated multiples. We carried out the estimation of the thin-bed parameters in the frequency (amplitude spectrum) domain using simulated annealing. In contrast to using zero-offset data, the use of AVA data contributes to increase the robustness of this inverse problem under noisy conditions, as well as to significantly reduce its inherent nonuniqueness. To further reduce the nonuniqueness, and as a means to incorporate a priori geologic or geophysical information (e.g., well-log data), we imposed appropriate bounding constraints to the parameters of the media lying above and below the thin bed, which need not be known accurately. We tested the method by inverting noisy synthetic gathers corresponding to simple wedge models. In addition, we stochastically estimated the uncertainty of the solutions by inverting different data sets that share the same model parameters but are contaminated with different noise realizations. The results suggest that thin beds can be characterized fully with a moderate to high degree of confidence below tuning, even when using an approximate wavelet spectrum.

INTRODUCTION

Extracting stratigraphic information from seismic data below the tuning thickness always has been a key objective for many geophysicists, used, for example, to characterize hydrocarbon-interbedded reservoirs. The conventional method to estimate bed thickness consists of measuring the time difference between the peak and trough of the seismic response. As is well known, this procedure is not appropriate to estimate the thickness for layers below tuning, unless it is combined with a thoughtful analysis of seismic amplitudes, which requires wavelet-phase knowledge (Widess, 1973; Kallweit and Wood, 1982). Moreover, the Widess model assumes that the reflection coefficients are equal and opposite.

Thus, for subtuning thicknesses, some extra information contained in the data should be taken into account. Spectral decomposition (Partyka et al., 1999; Marfurt and Kirlin, 2001), for example, uses the discrete Fourier transform of the data to map time thicknesses. Essentially, the notch spacing in the amplitude spectrum is associated with the reflection coefficients' time differences, and therefore to bed time thickness. The primary limitation of spectral decomposition is data bandwidth because these notches might not be identifiable for subtuning thicknesses.

Recently, Puryear and Castagna (2006, 2008) proposed a spectral inversion algorithm that can provide robust time-thickness estimates below tuning by inverting the amplitude spectrum of the thin-bed zero-offset seismic response. The reflection coefficients are estimated also, leading to a sparse-reflectivity inversion. Although robust and accurate, the method relies on the reflectivity model and is aimed to obtain the time thickness and the reflection coefficients alone. To fully determine the thin-bed parameters (including thickness in length units, compressional and shear-wave velocities, and density), which subsequently could be used to derive useful lithology and fluid information, it is clear that the information contained in the reflectivity-based zero-offset seismic trace is insufficient. A more complete modeling of the seismic response of the thin bed is required.

These facts encouraged us to propose a different methodology to characterize thin beds using the amplitude spectra of prestack data, because amplitude-versus-angle (AVA) anomalies are expected to exist (Liu and Schmitt, 2003). This extra information increases the robustness of the inversion and reduces its inherent nonuniqueness, permitting us to fully determine the thin-bed thickness and physical parameters. Although a priori information about the media lying above and below the thin bed is needed, it need not be known accu-

Manuscript received by the Editor 12 June 2008; revised manuscript received 23 December 2008; published online 30 June 2009.
[1]Universidad Nacional de La Plata, Facultad de Ciencias Astronómicas y Geofísicas, La Plata, Argentina, and CONICET, Argentina. E-mail: grubino@fcaglp.unlp.edu.ar; velis@fcaglp.unlp.edu.ar.

rately. Furthermore, the proposed algorithm improves the estimation of their properties.

It is worth mentioning that our methodology does not require any phase information, which is an advantage in many cases. Only an estimate of the amplitude spectrum of the wavelet is needed to simulate the AVA spectral response of the thin bed. In addition, because the proposed technique relies entirely on the amplitude spectra of the data, normal-moveout (NMO) corrections are not required; then, stretching effects have no implications. In this regard, it is assumed that the thin-bed seismic response in the amplitude-versus-offset (AVO)/AVA domain can be isolated by using an appropriate angle-dependent time window. Some additional practical issues must be taken into account. In this sense, the method assumes plane-wave propagation, planar interfaces, known estimates of the properties of the media lying above and below the thin bed, and decomposition of the data into angle-time domain.

The numerical experiments suggest that all the thin-bed parameters can be determined with a reasonable uncertainty, even when only an approximate wavelet amplitude spectrum is available. The examples include two models that simulate high- and low-velocity gas-sand layers embedded between two encasing half-spaces. Wedge models are used to test the algorithm for thicknesses below and above tuning.

METHODOLOGY

AVA response of a thin bed

The seismic response of real thin-bed reservoirs is very complex, and it usually is affected by undesired signals associated with the over- and underburdens. Despite this, we assume a simplified model in which these effects are neglected, which allows us to obtain useful information for characterizing these environments. In this sense, we consider a plane compressional wave striking at an elastic, horizontal, thin layer embedded between two homogeneous half-spaces. To obtain the AVA response of the thin bed, we follow the methodology presented by Liu and Schmitt (2003), but we include the propagation of shear waves generated at the layer interfaces.

Let a plane, harmonic, compressional wave of frequency $\omega = 2\pi f$ and unit amplitude propagate in the (x,z) plane, arriving at the thin bed with an incidence angle θ (see Figure 1). The particle displacements in the top half-space are caused by the contributions of the incident wave, and the reflected compressional and shear perturbations; whereas, in the bottom half-space, they are given by the superposition of the particle displacements generated by the transmitted compressional and shear waves. On the other hand, the displacements within the thin bed are obtained by considering four partial wavefields associated with a compressional and a shear wave traveling upward, and a compressional and a shear wave traveling downward within the thin bed.

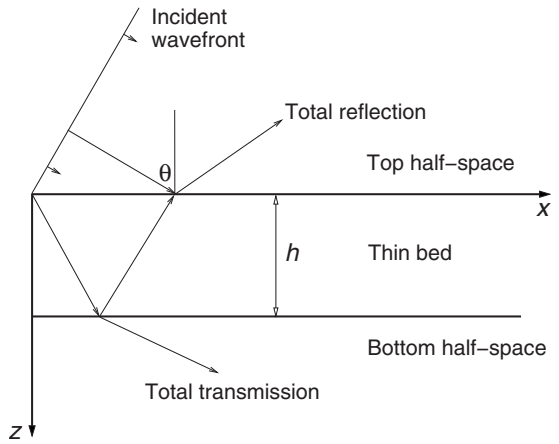

Figure 1. Diagram of the thin-bed model, and reflection and transmission rays. For simplicity, we do not show the shear waves generated at the interfaces, which indeed are included in the AVA response calculations.

To represent the different contributions, we use scalar and vector potentials associated with compressional and shear perturbations, respectively. The scalar potentials in the top half-space, thin layer, and bottom half-space can be written, respectively, as

$$\begin{aligned}\phi_1 &= e^{i(\omega t - k^p_{x_1} x - k^p_{z_1} z)} + R_p(\omega) e^{i(\omega t - k^p_{x_1} x + k^p_{z_1} z)},\\ \phi_2 &= A_p(\omega) e^{i(\omega t - k^p_{x_2} x - k^p_{z_2} z)} + B_p(\omega) e^{i(\omega t - k^p_{x_2} x + k^p_{z_2} z)},\\ \phi_3 &= T_p(\omega) e^{i(\omega t - k^p_{x_3} x - k^p_{z_3} z)},\end{aligned} \tag{1}$$

where $R_p(\omega)$ and $T_p(\omega)$ are the generalized compressional reflection and transmission coefficients, respectively, and $A_p(\omega)$ and $B_p(\omega)$ are the amplitudes of the contributions to the scalar potential within the thin bed. In addition, $\mathbf{k}^p_i = (k^p_{x_i}, \pm k^p_{z_i})$ are the wave vectors associated with the compressional perturbations in the top half-space $(i = 1)$, thin bed $(i = 2)$, and bottom half-space $(i = 3)$. Their moduli are given by $k^p_i = \omega / V_{p_i}$, where V_{p_i} represents the compressional velocities.

The vector potentials, associated with the shear perturbations in the different media, are given by

$$\begin{aligned}\psi_1 &= R_s(\omega) e^{i(\omega t - k^s_{x_1} x + k^s_{z_1} z)} \breve{e}_2,\\ \psi_2 &= [A_s(\omega) e^{i(\omega t - k^s_{x_2} x - k^s_{z_2} z)} + B_s(\omega) e^{i(\omega t - k^s_{x_2} x + k^s_{z_2} z)}] \breve{e}_2,\\ \psi_3 &= T_s(\omega) e^{i(\omega t - k^s_{x_3} x - k^s_{z_3} z)} \breve{e}_2.\end{aligned} \tag{2}$$

Here, $R_s(\omega)$ and $T_s(\omega)$ are the generalized shear reflection and transmission coefficients, respectively, and $\breve{e}_2$ denotes the unit vector along the y Cartesian axis. In addition, $A_s(\omega)$ and $B_s(\omega)$ are the amplitudes of the contributions to the vector potential within the thin layer. Expressions $\mathbf{k}^s_i = (k^s_{x_i}, \pm k^s_{z_i})$ are the wave vectors associated with the shear perturbations in the different media, and their moduli are given by $k^s_i = \omega / V_{s_i}$, where V_{s_i} represents the shear velocities.

The particle displacements in the top half-space, thin bed, and bottom half-space, are given, respectively, by

$$\begin{aligned}\mathbf{u}^1 &= \nabla \phi_1 + \nabla \times \psi_1,\\ \mathbf{u}^2 &= \nabla \phi_2 + \nabla \times \psi_2,\\ \mathbf{u}^3 &= \nabla \phi_3 + \nabla \times \psi_3.\end{aligned} \tag{3}$$

Substituting equations 1 and 2 into equation 3, and requiring the continuity of the horizontal component of the particle displacement through the bottom and top layer interfaces, it is easy to conclude that

$$k^p_{x_1} = k^p_{x_2} = k^p_{x_3} = k^s_{x_1} = k^s_{x_2} = k^s_{x_3}, \tag{4}$$

which is Snell's law. Next, taking into account that $k^p_{x_1} = k^p_1 \sin\theta$, and using equation 4, we find that

$$k_{z_i}^{\alpha} = [(k_i^{\alpha})^2 - (k_1^p \sin\theta)^2]^{1/2}, \quad \alpha = p,s \quad i = 1,2,3. \quad (5)$$

Then, using the elastic properties of each medium, we relate the displacement vectors with the stress tensors by means of Hooke's law. As usual, we require the continuity of the displacements and normal and shear stresses through the top and bottom layer interfaces, which leads to an 8×8 linear system of equations, where the unknowns are the eight potential amplitudes.

The product of the source amplitude spectrum and the modulus of the potential amplitude $R_p(\omega)$ for different incidence angles, constitutes the amplitude spectra of the prestack data. This methodology allows us to calculate the seismic response of a plane compressional wave arriving at a thin layer in the angle-frequency (amplitude spectrum) domain. The modeling takes into account the effects of converted P-waves, S-waves, and all the associated multiples generated at the layer interfaces. Should the source phase be available, the seismic response in the angle-time domain could be obtained.

Prestack spectral inversion

Let $A(f,\theta)$ and $\hat{A}(f,\theta)$ be the amplitude spectra of the observed and calculated prestack data, respectively. In practice, the thin-bed seismic response should be identified first, and then isolated by using an angle-dependent time window. This window is centered at the thin-bed response and is of constant length. Next, $A(f,\theta)$ is obtained by applying the Fourier transform to the windowed data after applying a taper (e.g., a Hamming window) to minimize truncation errors. Notice here that wavelet phase and NMO corrections are not required, which represents an advantage of the proposed method.

We define cost function J, as a 10-dimensional function that depends on the elastic properties and densities of the top and bottom half-spaces, and on the thickness, density, and elastic properties of the thin bed. It is given by

$$J = \frac{1}{NM} \sum_{i=1}^{N} \sum_{j=1}^{M} w_i [A(f_j,\theta_i) - \hat{A}(f_j,\theta_i)]^2, \quad (6)$$

where N is the number of angles of the prestack data, M is the number of frequencies utilized, and w_i are weights. For simplicity, in the examples below, we selected all weights equal to one.

Clearly, the problem of finding the set of model parameters that minimize J represents a highly nonlinear inverse problem. To avoid local minima and poor convergence, we minimize J using a hybrid optimization scheme that involves both simulated annealing (SA) and a linearizing approach. In practice, we minimize J using very fast simulated annealing (Ingber, 1989) for a fixed number of iterations until convergence to the global minimum region. Then we switch to the linearizing stage (we use the Powell's quadratically convergent method as described in Press et al., 1992) to refine the solution and accelerate convergence to the global minimum. We incorporate bounding constraints in all the model parameters to guarantee physically reasonable models. The possibility of fixing a given search range for each model parameter individually is very convenient to force the solution to honor any available a priori geologic or geophysical information (e.g., well-log data). In a practical context, this contributes to reduce the nonuniqueness of the inverse problem.

Table 1. High- and low-velocity gas-sand models.

Model	Layer	V_p (km/s)	V_s (km/s)	ρ (gr/cm^3)
High	top	3.094	1.515	2.40
	middle	4.050	2.526	2.21
	bottom	3.146	1.554	2.41
Low	top	3.048	1.244	2.40
	middle	2.438	1.626	2.14
	bottom	3.048	1.244	2.46

SIMULATION RESULTS AND DISCUSSION

To analyze the behavior of the proposed prestack spectral inversion method in various geologic thin-bed scenarios, we invert the simulated AVA spectral data corresponding to two different models: a high- and a low-velocity layer embedded between two half-spaces. The parameters that describe these two models are defined in Table 1. The low-velocity model corresponds to the classical Ostrander gas-sand model (Ostrander, 1984); whereas, the high-velocity model also represents a gas-sand model (Nowak et al., 2008), with encasing shales on top and bottom.

In both cases, we use wedge models with thicknesses varying from 0.1 through 1.5 times the tuning thickness. The tuning time thickness for a Ricker wavelet is $\sqrt{6}/(2\pi f_0)$, where f_0 is the dominant frequency (Chung and Lawton, 1995). For generating the AVA data, we select a 30-Hz Ricker wavelet, which leads to a tuning thickness of about 13 ms. In terms of length units, this value corresponds to layers of 16 and 26 m for the low- and high-velocity models, respectively. The simulated data (21 traces per gather) take into account incidence angles ranging from 0° through 40° in all cases. We then contaminate the resulting gathers with additive Gaussian noise with a given signal-to-noise ratio (S/N). We define the S/N as the ratio between the noise-free gather energy and the noise energy. For the minimization of J, we select a frequency band where the S/N is expected to be higher (10–60 Hz).

To assess the uncertainty associated with the model parameter estimations, we repeat the inversion for 100 different data sets that share the same model parameters, but are contaminated with different noise realizations. Then we calculate the uncertainty by averaging all the individual solutions and computing the standard deviations.

The problem of nonuniqueness

Figure 2 shows the simulated gather and associated amplitude spectra corresponding to the high-velocity model, for a very thin layer with $h = 8$ m and S/N = 100. There is a noticeable decrease in the amplitude of the seismic response and a change in the character of the signal, as interbed multiples and wave mode conversions develop for different incidence angles. A time-domain picking of the peak and trough of the zero-offset trace yields a time difference of about 12 ms, a value that corresponds to a thickness of approximately 24 m, which is three times the actual value. Naturally, this is a very inaccurate estimation, and results from the fact that the information contained in the peak-trough time difference is useless below tuning.

Another approach to characterize thin beds is the spectral inversion method proposed by Puryear and Castagna (2008). It is based on zero-offset data and targets reflection coefficients and time thicknesses. It would be interesting to see whether the amplitude spectra of zero-offset data provide the additional information needed to determine the thickness (in length units) and reasonable estimates of the velocities and densities. Figure 3a shows the logarithm of the cost function J using only the amplitude spectrum of the zero-offset trace for the high-velocity model (8-m-thick bed), fixing all parameters to their actual values except h and V_p. Clearly, there are many model parameters that yield an amplitude spectrum that fits the data. The higher-velocity family of solutions essentially produces seismic responses very similar to the true data. The lower-velocity family of solutions yields time-reversed seismic responses, with an amplitude spectrum similar to that of the true data. In sum, there is an inherent ambiguity which shows that the information contained in the spectra of zero-offset data is not sufficient to estimate all the mentioned parameters simultaneously.

On the other hand, when using the amplitude spectra of the prestack data ($N = 21$, θ in the range of 0–40°), cost function J clearly shows an isolated minimum around the actual model parameters (Figure 3b). Thus, the use of prestack information is essential to significantly reduce the nonuniqueness of the inverse problem, further suggesting that these data could be used to effectively determine all the thin-bed properties.

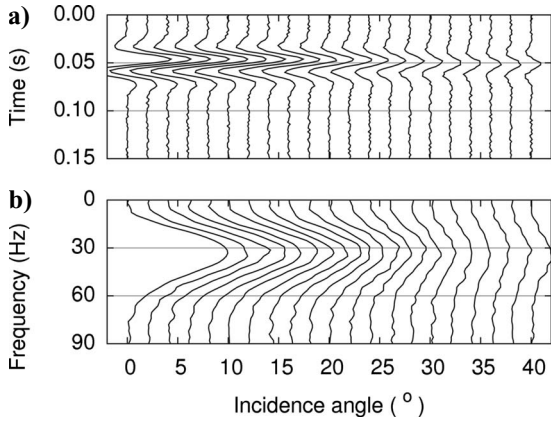

Figure 2. (a) Simulated gather, and (b) amplitude spectra for the high-velocity model ($h = 8$ m, S/N = 100).

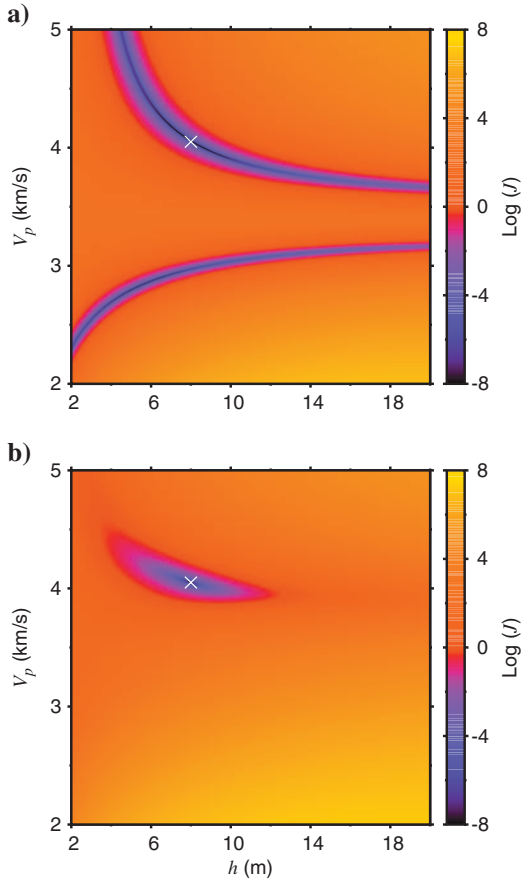

Figure 3. Log(J) as a function of thickness h and V_p in the high-velocity model: (a) using only the amplitude spectrum of the zero-offset trace; (b) using the amplitude spectra of the whole gather. The white cross indicates the true solution $(h,V_p) = (8.0,4.05)$. Note that all remaining parameters were fixed to their true values.

High-velocity gas-sand model

Figure 4 shows the results of the full spectral inversion of the prestack data for the high-velocity wedge model. We assume that the elastic parameters and densities of the top and bottom half-spaces are known within a given tolerance error. That is, the SA search is performed over a wide search range for the thin-bed parameters (the search ranges coincide with the y-axes' limits in the plots), but a narrower search range is allowed for the parameters of the two half-spaces. Figure 4a shows the results when the half-space parameters are allowed to be adjusted in the range given by the true values $\pm$ 1%. In Figure 4b and c, these ranges are increased to $\pm$ 10%. In addition, the data are contaminated with noise, using S/N = 100 in Figure 4a and b, and S/N = 10 in Figure 4c.

In the three cases, the results are very accurate, with mean relative errors below 10% in most cases. The uncertainty of the thickness estimates is very small, even for thicknesses far below tuning and when top and bottom parameters are known only within 10% tolerance. As expected, for thicknesses above tuning, the accuracy of the estimates increases significantly, except for density in Figure 4b and c. Even in the case of higher S/N, the results show that thin beds of a few meters can be characterized very well.

Besides the characterization of the thin bed, this process also involves the adjustment of the top and bottom half-space parameters through a restricted search around some a priori estimates. Such search ranges must not be too wide, because they could lead to ambiguities that are difficult to resolve even using the full gather. However, for the selected search ranges ($\pm$ 10%), results demonstrate that the estimation of these parameters (not shown) is very accurate. In practice, the uncertainties of these estimates are much smaller than the $\pm$ 10% tolerance specified for their respective search ranges, giving additional information to improve the knowledge of the geologic setting.

For illustrative purposes, Figure 5 shows the estimated gather for $h = 8$ m as compared to the actual data. The estimated gather was

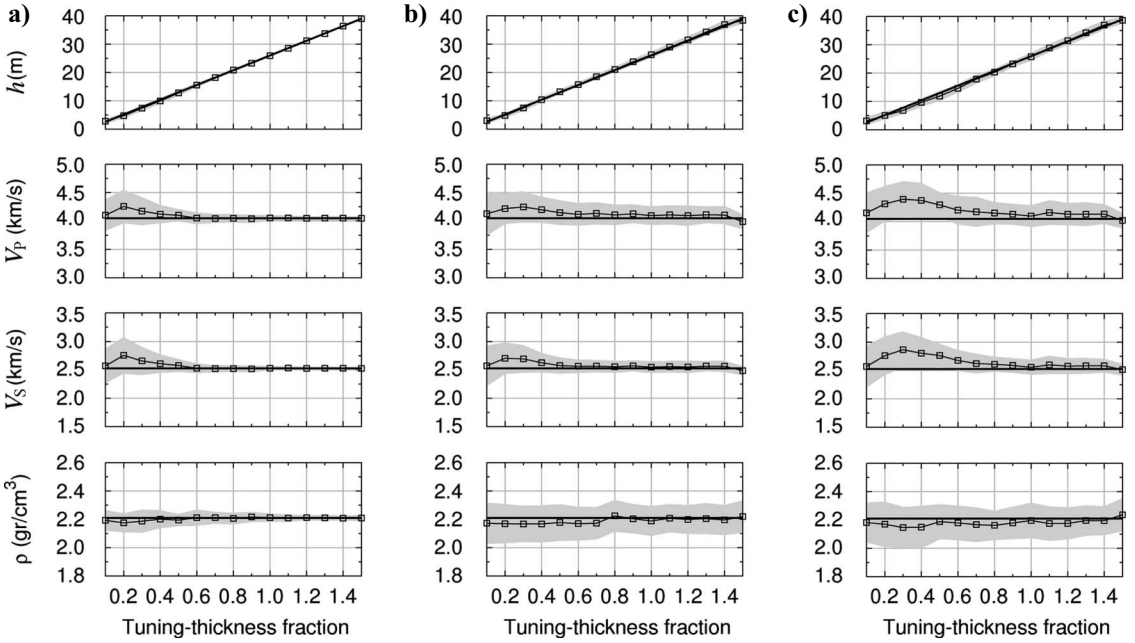

Figure 4. Prestack spectral inversion in the high-velocity wedge model. Top and bottom half-space parameters are known within a 1% tolerance error in column (a), and 10% in columns (b) and (c). Data with S/N = 100 in (a) and (b), and S/N = 10 in (c). The plots show the mean solution (squares) plus or minus one standard deviation (shaded area). Solid black lines show actual values. Tuning-thickness fraction of 1.0 corresponds to 26 m.

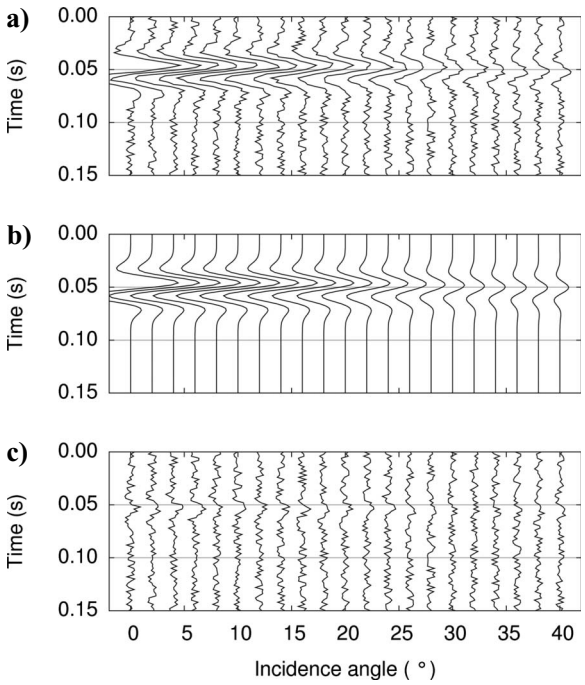

Figure 5. (a) Actual gather for the high-velocity model (h = 8 m, S/N = 10). (b) Calculated gather after the inversion using the mean model parameters. (c) Residual.

generated using the mean parameters shown in Figure 4c, for a tuning thickness fraction of about 0.3. The residual in Figure 5c shows that the fit is very good, considering we are determining the parameters of a bed as thin as 8 m using noisy data. In addition, Figure 6 illustrates the observed and estimated traces and amplitude spectra for $\theta = 0$ and 40°, showing an excellent agreement between observed and calculated data.

Low-velocity gas-sand model

The results of the prestack spectral inversion for a wedge model, with thicknesses varying from 0.1 through 1.5 of the tuning thickness (i.e., 1.6–24 m), and for the case of the low-velocity model, are shown in Figure 7. We can observe that uncertainties of the various parameter estimates are higher than in the high-velocity model, although the accuracy is very good, with mean relative errors below 10–15% in most cases. In this case also, the model parameter with higher uncertainty is density, meaning that it is not very well resolved with the information contained in the gather. Nonetheless, it is determined with accuracies below 10% in most cases. Although in general, the uncertainties of all the parameters increase in the higher-noise case, the results show that thin beds of a few meters can be characterized very well.

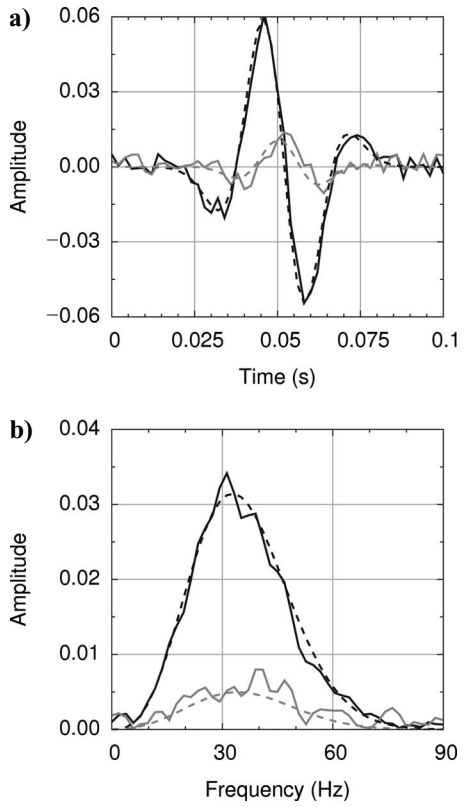

Figure 6. (a) Seismic responses, and (b) amplitude spectra for an 8-m-thick bed, for $\theta = 0°$ (solid black) and $\theta = 40°$ (solid gray) in the high-velocity model. Top and bottom half-space parameters are known within a 10% tolerance error, and S/N = 10. Dashed lines show the calculated data using the mean parameter estimates after the full prestack spectral inversion.

The general increase in the uncertainty of the parameters is associated with a decrease in the amount of information contained in the data. In effect, Figure 8a shows the data corresponding to a thin bed of 4.8 m: the AVA effect is much smaller than in the high-velocity case (Figure 5a).

For the sake of completeness, Figure 8b and c shows the estimated gather using the mean model parameters and the residual, respectively. Finally, Figure 9 depicts the observed and estimated traces and amplitude spectra for $\theta = 0°$ and 40°, showing an excellent agreement between observed and calculated data. For this plot, we selected $h = 4.8$ m, which represents 27% of the tuning thickness. Note the high noise levels in the data (spectra) used for the inversion.

Sensitivity to wavelet spectrum

In the previous examples, we assumed that the amplitude spectrum of the wavelet was known accurately. Here, we show how the prestack spectral inversion method behaves when only an approximate wavelet spectrum is available.

For this purpose, we generate an approximate amplitude spectrum by contaminating the actual wavelet in time domain with filtered random noise, and calculating the magnitude of its Fourier transform. Figure 10 shows the amplitude spectrum of the actual 30-Hz Ricker wavelet used in the simulation of the data, along with the amplitude spectrum of the noisy wavelet used for the inversion in the following examples.

Figure 11 shows the results of the inversion in the (a) high- and (b) low-velocity wedge models, using noisy data (S/N = 10). As expected, the uncertainty in the estimation of the model parameters increases significantly, especially for the low-velocity model, where the information content of the gathers is lower. Nevertheless, in most cases, the estimated parameters are within 10% of the true values, except for the smallest thicknesses. These figures are to be compared to Figures 4c and 7c, respectively. Although there is an overall decrease in the quality of the results, the spectral inversion procedure still can provide useful information to characterize thin beds.

It is worth mentioning that the inverse problem is poorly constrained in these examples, because no information is provided to restrict the search of the thin-bed parameters. Note that the search ranges are very wide (y-axes in the plots), allowing for variations of density of more than 50% of the true value, and variations of velocities of more than 100% in some cases. The search range for thickness goes from 2 m through 40 m, and from 2 m through 25 m in the high- and low-velocity models, respectively, independently of the true thickness. Should well-log data be available, one or more parameters could be restricted to a narrower search range, and the uncertainty (and the inverse problem nonuniqueness) would be reduced significantly. Furthermore, the information content of the data could be increased by using more traces (i.e., beyond 40°). The presented forward modeling has no limitations in this sense. However, the errors associated with the mapping of the data into the required angle-time domain would certainly increase for larger angles. In addition, there also will be more interferences, so the model assumptions might become less appropriate.

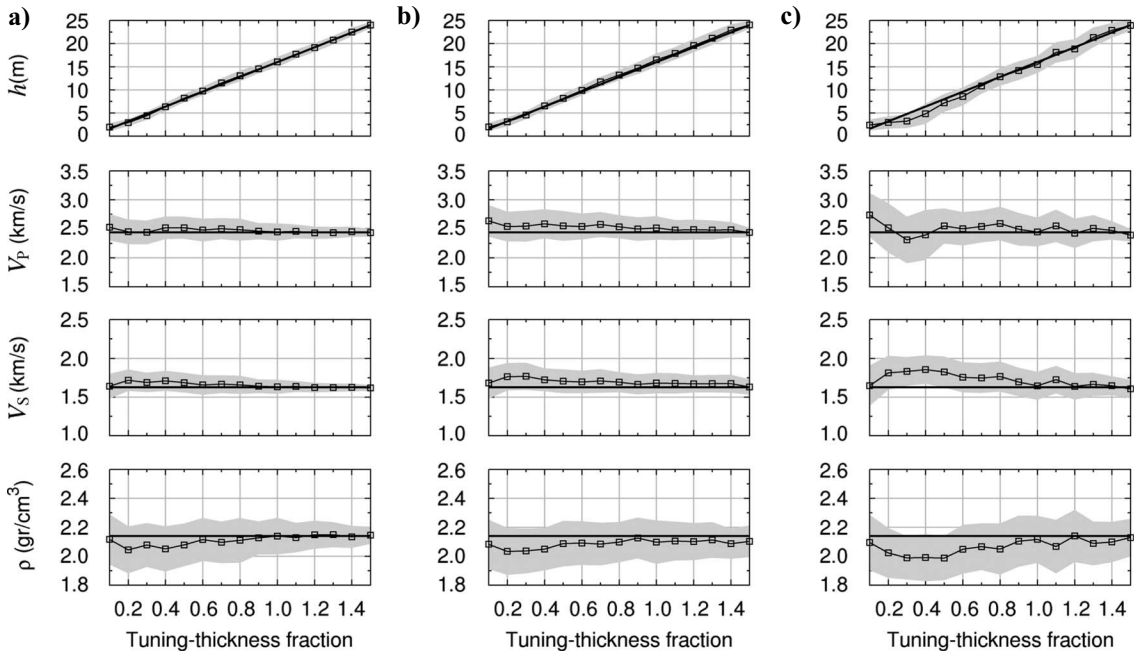

Figure 7. Prestack spectral inversion in the low-velocity wedge model. Top and bottom half-space parameters are known within a 1% tolerance error in column (a), and 10% in columns (b) and (c). Data with S/N = 100 in (a) and (b), and S/N = 10 in (c). The plots show the mean solution (squares) plus or minus one standard deviation (shaded area). Solid black lines show actual values. Tuning thickness fraction of 1.0 corresponds to 16 m.

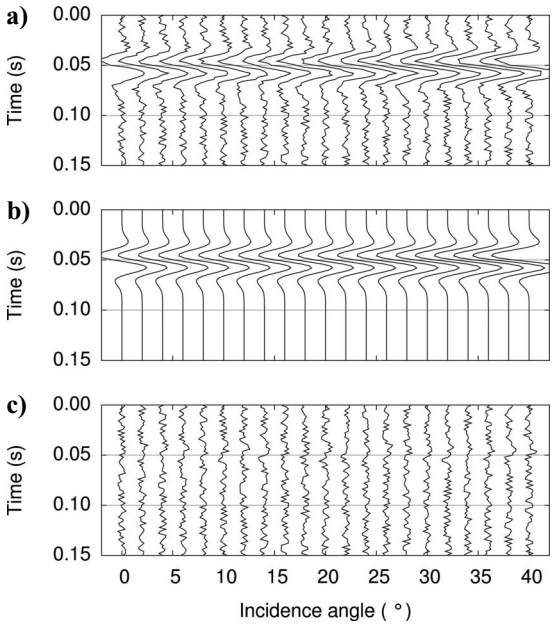

Figure 8. (a) Actual gather for the low-velocity model (h = 4.8 m, S/N = 10). (b) Calculated gather after the inversion using the mean model parameters. (c) Residual.

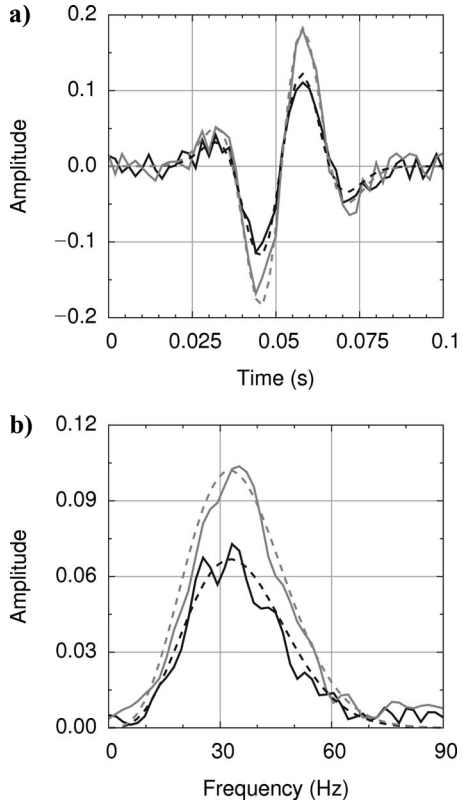

Figure 9. (a) Seismic responses, and (b) amplitude spectra for a 4.8 -m-thick bed, for $\theta = 0°$ (solid black) and $\theta = 40°$ (solid gray) in the low-velocity model. Top and bottom half-space parameters are known within a 10% tolerance error, and S/N = 10. Dashed lines show the calculated data using the mean parameter estimates after the full prestack spectral inversion.

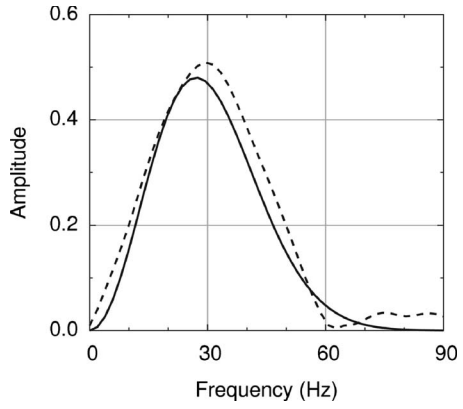

Figure 10. Wavelet amplitude spectra: true spectrum (solid), and approximate spectrum (dashed).

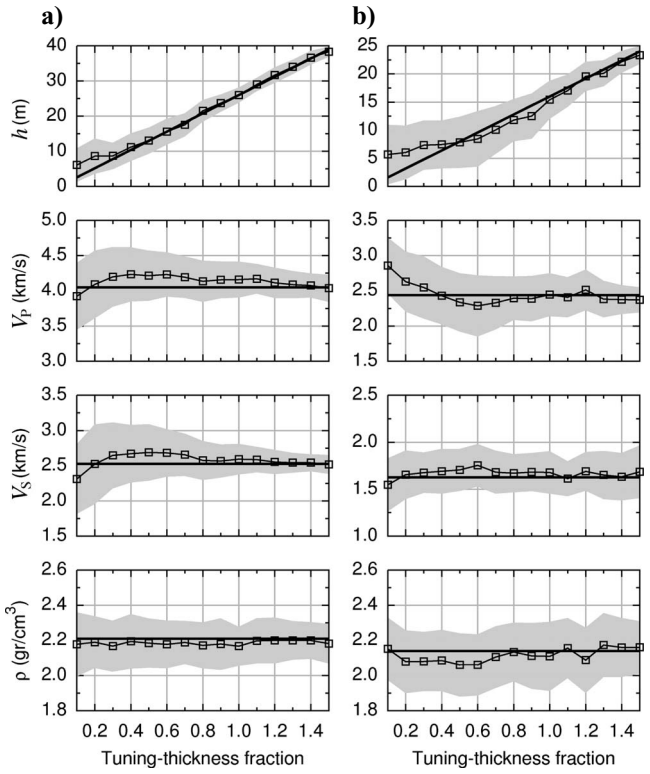

Figure 11. Prestack spectral inversion in the high- (a) and low-velocity (b) wedge models, when using an approximate wavelet amplitude spectrum. Top and bottom half-space parameters are known within a 10% tolerance error, and S/N = 10. The plots show the mean solution (squares) plus or minus one standard deviation (shaded area). Solid black lines show actual values. Tuning thickness fraction of 1.0 corresponds to 26 m and 16 m, respectively.

CONCLUSIONS

The amplitude spectrum of zero-offset data does not provide enough information to determine the thin-bed thickness (in length units) and its elastic parameters simultaneously, because there are many inherent ambiguities that cannot be resolved. On the contrary, the amplitude spectra of prestack data provide enough information to determine all the thin-bed parameters, including thickness, density, and compressional and shear velocities. In a practical context, the fact that the method requires neither phase information nor NMO corrections constitutes an advantage. At the same time, the procedure allows one to adjust the estimates of the elastic properties and densities of the media lying above and below the thin bed. The use of SA permits us to solve the highly nonlinear constrained optimization problem associated with the inversion of the prestack data. The results using simulated noisy data are encouraging because they suggest that beds as thin as a few meters can be characterized fully with a reasonable uncertainty and accuracy. When only an approximate wavelet amplitude spectrum is available, the results still are robust under noisy conditions, especially when data show a significant AVA anomaly.

We believe that this methodology could be adapted to encompass multiple layers. This issue and the application of the inversion procedure to real data will be considered in future works.

ACKNOWLEDGMENTS

This work was partially financed by Universidad Nacional de La Plata, Argentina, Agencia Nacional de Promoción Científica y Tecnológica (PICT 03-13376) and CONICET (PIP 04-5126).

REFERENCES

Chung, H., and D. Lawton, 1995, Frequency characteristics of seismic reflections from thin beds: Canadian Journal of Exploration Geophysicists, **31**, 32–37.

Ingber, L., 1989, Very fast simulated re-annealing: Journal of Mathematical Computation and Modelling, **12**, 967–973.

Kallweit, R. S., and L. Wood, 1982, The limits of resolution of zero-phase wavelets: Geophysics, **47**, 1035–1046.

Liu, Y., and D. R. Schmitt, 2003, Amplitude and AVO responses of a single thin bed: Geophysics, **68**, 1161–1168.

Marfurt, K., and R. Kirlin, 2001, Narrow-band spectral analysis and thin-bed tuning: Geophysics, **66**, 1274–1283.

Nowak, E. J., H. W. Swan, and D. Lane, 2008, Quantitative thickness estimates from the spectral response of AVO measurements: Geophysics, **73**, no. 1, C1–C6.

Ostrander, W. J., 1984, Plane-wave reflection coefficients for gas sands at nonnormal angles of incidence: Geophysics, **49**, 1637–1648.

Partyka, G., J. Gridley, and J. Lopez, 1999, Interpretational applications of spectral decomposition in reservoir characterization: The Leading Edge, **18**, 353–360.

Press, W. H., S. Teukolsky, W. Vetterling, and B. Flannery, 1992, Numerical recipes in FORTRAN: The art of scientific computing, 2nd ed.: Cambridge University Press.

Puryear, C. I., and J. P. Castagna, 2006, An algorithm for calculation of bed thickness and reflection coefficients from amplitude spectrum: 76th Annual International Meeting, SEG, Expanded Abstracts, 1767–1770.

———, 2008, Layer-thickness determination and stratigraphic interpretation using spectral inversion: Theory and application: Geophysics, **73**, no. 2, R37–R48.

Widess, M., 1973, How thin is a thin bed?: Geophysics, **38**, 1176–1180.